

Kraft lignin and polyethylene terephthalate blends: effect on thermal and mechanical properties

Livia Lazzari¹, Eloilson Domingos^{1,2}, Leticia Silva^{3,4}, Alexei Kuznetsov³, Wanderson Romão^{1,2} and Joyce Araujo^{3*} 

¹Laboratório de Química Analítica, Instituto de Química, Instituto Federal de Educação, Ciência e Tecnologia do Espírito Santo – IFES, Vila Velha, ES, Brasil

²Laboratório Petrolômico e Forense, Departamento de Química, Universidade Federal do Espírito Santo – UFES, Vitória, ES, Brasil

³Divisão de Metrologia de Materiais, Instituto Nacional de Metrologia, Qualidade e Tecnologia – Inmetro, Duque de Caxias, RJ, Brasil

⁴Universidade Federal do Rio de Janeiro – UFRJ, Duque de Caxias, RJ, Brasil

*jraraujo@inmetro.gov.br

Abstract

In this work, bottle-grade poly(ethylene terephthalate) (PET_R), kraft lignin (KL), and chemically modified lignin (ML) were used to form blends to improve the mechanical and thermal properties of pure PET. The PET/KL and PET_R/ML blends were produced with 0.5, 1, 3, and 5 wt.% of lignin via melt extrusion and injection molding. The produced blends and PET_R were characterized by Fourier transform infrared spectroscopy (FTIR), thermogravimetry (TGA), differential scanning calorimetry (DSC) and mechanical properties testing. The FTIR measurements confirmed the chemical modifications of the ML samples, while the TGA results showed KL to be thermally more stable than ML. The glass transition temperature of PET_R changed as a function of the amount of lignin, as revealed by the DSC measurements. The PET/KL blends demonstrated their potential for use as an engineering material due to their improved thermal and mechanical properties compared to those of PET_R.

Keywords: blends, kraft lignin, mechanical properties, poly(ethylene terephthalate).

How to cite: Lazzari, L., Domingos, E., Silva, L., Kuznetsov, A., Romão, W., & Araujo, J. (2019). Kraft lignin and polyethylene terephthalate blends: effect on thermal and mechanical properties. *Polímeros: Ciência e Tecnologia*, 29(4), e2019055. <https://doi.org/10.1590/0104-1428.06618>

1. Introduction

Synthetic or petroleum-based polymers have many practical uses; however, their low biodegradability causes serious environmental problems. Consequently, several strategies to replace or reduce the use of synthetic polymers have been developed^[1-4]. Sustainable development requirements open new perspectives for products obtained from polymer recycling processes, as they significantly contribute to a reduction in plastic waste^[5].

Polyethylene terephthalate (PET) is a semi-crystalline thermoplastic aromatic polyester known for its mechanical properties, lightness, strength, and high transparency, which ensure its widespread use in food and cosmetic packaging materials^[2,6-10]. Currently, recycled PET is often mixed with other polymers or fillers to produce polymer blends or composites with different mechanical and thermal properties compared to neat polymers, thus adding value to raw materials. For added-value processes to be consistently efficient, the compatibility between mixture components is highly essential to achieve satisfactory thermal and mechanical properties for a specific application^[11-13]. Mechanical enhancements may be useful to the automobile and civil construction industries,

while improvements of thermal stability would be useful for applications in the packaging and electronics industries.

Lignin is one of the three main constituents of a plant. It is the second most abundant polymer in the world after cellulose. Generally, its structure depends on the species of wood and the processing conditions. Kraft, sulfite, and soda are the main processes used in chemical wood pulping for extracting cellulose from wood by dissolving the lignin that binds the cellulose fibers together^[14,15].

The kraft pulping process involves digesting wood chips and moiled paper at elevated temperature and pressure in a water solution of sodium sulfide and sodium hydroxide, called “white liquor.” The white liquor chemically dissolves the lignin that binds the cellulose fibers together. Spent “white liquor,” containing suspended particulate solids and organic compounds, is concentrated to a mostly solid pulp, called “black liquor,” which contains between 10 to 50 wt.% of dissolved lignin^[14,16,17]. Today, most of the lignin produced by the pulp and paper industry as a constituent part of the black liquor by-product is burned to provide heat for electric power generation. However, as lignin is a complex polyfunctional

macromolecule composed of a large number of polar functional groups, it has the potential for use in several technological applications and can be used to produce high-added-value products^[18-20].

Blending lignin with a polymeric matrix is a secure way to develop polymer-based products with desirable properties. However, the eventual incompatibility on a chemical level between the components may require the chemical modification of lignin before mixing to improve its dispersion in plastic or to increase interfacial adhesion^[14,17,21,22].

This work aimed to develop a new engineering material with enhanced mechanical and thermal properties using waste PET bottles and lignin, which was obtained as a by-product of the kraft process. The PET/lignin blends were produced by melt extrusion and injection molding and contained chemically modified and unmodified lignin. The thermal and mechanical properties of the blends were compared with those of the PET_R matrix.

2. Materials and Methods

2.1 Materials

Lignin from the kraft process, referred to here as KL, was supplied by Fibria Celulose S/A (São Paulo, Brazil). Chemical modification of the lignin was accomplished using ethylic alcohol 95% (v/v) (CAS 64-17-5), sodium hydroxide 97% (wt/wt) (CAS 1310-73-2), and monochloroacetic acid 99% (wt/wt) (CAS 79-11-8), all supplied by Sigma Aldrich.

Lignin was extracted from the black liquor via a precipitation method that consisted of the following steps: reduction of the liquor pH value (start solution was pH >13) with CO₂ injection, filtration of the precipitated lignin, suspension of the filtered lignin in a H₂SO₄ solution (pH 2.5), and filtration and washing of the lignin with an acidic solution (pH 2.5 and 60 °C).

The bottle-grade PET (PET_R) was obtained by grinding colorless PET bottles in a Retsch mill (model SM300) with a 2 mm sieve and 1500 rpm rotation. Prior to milling, the bottle labels were removed, and the areas with glue residue were cleaned.

2.2 Lignin modification

The lignin modification was performed as described by Silva et al.^[23]. Briefly, 10.0 g of lignin was suspended in 270 mL of 95% ethanol (v/v) under continuous stirring in a mechanical stirrer (Ethik Technology, model 105) to

which 27 mL of a 30% NaOH aqueous solution (wt/v) was added at a rate of 1 mL min⁻¹ using an electronic pipette (Transferpette S) at room temperature. After the addition of the NaOH solution, the final solution was stirred for a further 60 min. Subsequently, 12.0 g of monochloroacetic acid was gradually added over the course of 30 min, without further agitation of the solution. The mixture was then stirred for an additional 210 min at 55 °C. The residue was suspended in 670 mL of 95% ethanol solution (v/v), which was neutralized with glacial acetic acid, and the separated product was filtered. After filtration, the product was washed three times with approximately 50 mL of 95% ethanol (v/v) to remove the impurities and by-products and then dried at 60 °C in an oven until a constant mass was achieved. The modified lignin is denominated in this work as ML^[23].

2.3 Specimen preparation

Milled PET_R, KL, and ML samples were dried in a vacuum oven at 60 °C for 24 h prior to melting extrusion and injection molding.

The PET_R/lignin blends were fabricated by extrusion using a Thermo Scientific Haake MiniLab II extruder (processing temperature 275 °C and screw rotation speed 100 rpm). The reference specimens (PET_R) and its blends were injected into a Thermo Scientific Haake MiniJet II injector (injection temperature 275 °C, injection pressure 450 bar, injection time 4 s and molding temperature 25 °C). Table 1 displays the formulations of the specimens.

2.4 FTIR

The attenuated total reflectance Fourier transform infrared (ATR-FTIR) spectra were obtained on a Frontier spectrometer from Perkin Elmer. Each spectrum was recorded as the mean of 16 consecutive scans, with a resolution of 4 cm⁻¹ in a working range of 4000 to 630 cm⁻¹.

2.5 Thermogravimetry (TGA)

Thermogravimetry analysis (TGA) was performed on an SDT Q600 from TA Instruments. Approximately 10 mg of the sample was heated in the alumina crucible (25 °C to 900 °C) at a heating rate of 10 °C min⁻¹ under a nitrogen flow of 20 mL min⁻¹.

2.6 Differential Scanning Calorimetry (DSC)

Differential scanning calorimetry (DSC) was carried out using a TA Instruments Q200. Approximately 5 mg of the

Table 1. Composition of the formulations used to fabricate the tensile specimens.

Sample	PET _R (wt.%)	KL (wt.%)	ML (wt.%)	Formulation*
1	100	0	0	PET _R
2	99.5	0.5	0	PET/KF 0.5 wt.%
3	99	1.0	0	PET/KF 1.0 wt.%
4	97	3.0	0	PET/KF 3.0 wt.%
5	95	5.0	0	PET/KF 5.0 wt.%
6	99.5	0	0.5	PET/ML 0.5 wt.%
7	99	0	1.0	PET/ML 1.0 wt.%
8	97	0	3.0	PET/ML 3.0 wt.%
9	95	0	5.0	PET/ML 5.0 wt.%

* PET_R: bottle-grade poly(ethylene terephthalate), KL: kraft lignin, and ML: chemically modified lignin.

sample (injected material) was heated in the alumina crucible (25 °C to 400 °C) at a heating rate of 10 °C min⁻¹ under a nitrogen flow of 50 mL min⁻¹.

2.7 Tensile measurements

The tensile tests were performed according to the ISO 527-1:2012 (type 5A specimen) standard. The tests were conducted at the facilities of the Federal University of Espírito Santo (UFES)/LABPETRO using a Lloyd Instruments LR5K Plus universal testing machine. The measurement conditions were a load cell of 5 kN, a 50 mm strain gauge with a measurable deformation of 25 mm, and a crosshead speed of 1 mm min⁻¹.

3. Results and Discussion

3.1 ATR-FTIR

Figure S1a (see Supplementary Material) shows the ATR-FTIR spectra of the KL and ML samples, and the main bands and respective assignments are listed in Table 2 and Table 3. Figure S1a shows significant differences between

the ATR-FTIR spectra of ML and KL samples – one of them is the absence of the band at 1710 cm⁻¹ in the ML spectrum, exhibited by unmodified lignin (KL), which is attributed to the vibration of the carbonyl group conjugated to the aromatic ring. Instead, ML has two high-intensity bands, at 1598 and 1416 cm⁻¹, assigned to the carboxylate anion. The appearance of these intense bands demonstrates the efficiency of the carboxylation process in the modification reaction. The KL and ML samples both exhibited bands related to the stretching and in-plane bending of the CH₂ group, at 2938 and 1453 cm⁻¹, respectively, (Tabs. 2 and 3), indicating that these groups did not participate in the chemical reaction. The main bands of the PET_R polymer matrix as well as its PET_R/KL and PET_R/ML lignin blends are assigned in Table S1.

3.2 TGA

Figure 1a depicts the TGA curves of KL and ML. Mass losses of approximately 6 wt.% for KL and 22 wt.% for ML were observed at around 100 °C. This weight drop can be attributed to moisture loss. The chemical decomposition of KL and ML occurs over a wide temperature range, with the most intense mass loss being observed between 200 °C and

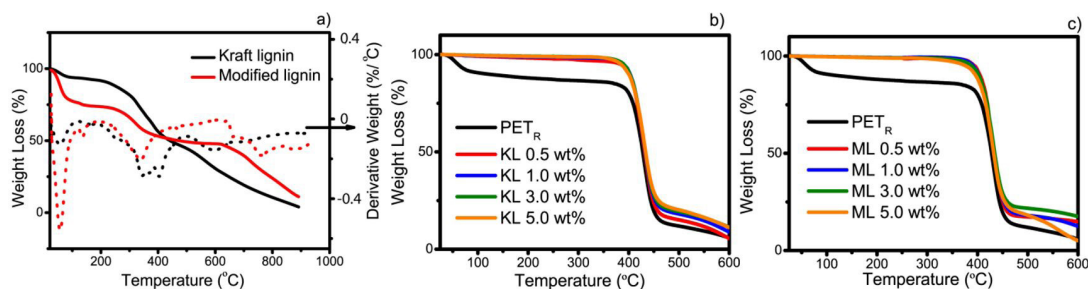


Figure 1. (a) TGA curves of the unmodified lignin (KL), modified lignin (ML), and PET_R and their own blends of (b) PET_R/KL and (c) PET_R/ML.

Table 2. Assignments of the vibrational bands of the lignin (KF)^[23-25].

Wavenumber (cm ⁻¹)	Assignment
3413	OH group (hydroxyl)
2934	aliphatic C-H asymmetric stretching
1710	C=O stretch of carboxylic acids, ketones, and aldehydes
1603	C=C aromatic stretching
1505	C=C aromatic stretching
1454	CH ₂ CH ₃ bending
1211	C-O phenolic stretching
1110	C-O stretching of the aliphatic secondary alcohol chain
1019	C-O stretching of the primary alcohol aliphatic chain

Table 3. Assignments of the vibrational bands of the modified lignin (ML)^[23-25].

Wavenumber (cm ⁻¹)	Assignment
3254	OH group (hydroxyl)
2938	aliphatic C-H asymmetric stretching
1598	asymmetric carboxylate stretching
1416	symmetrical carboxylate stretch
1507	C=C aromatic stretches
1453	CH ₂ CH ₃ bending
1249	C-O phenolic stretching
1123	C-O stretching of the aliphatic secondary alcohol chain
1031	C-O stretching of the primary alcohol aliphatic chain

700 °C. In this temperature range, KL loses approximately 72 wt.%, while ML loses about 34 wt.%^[23,26,27]. The wide range of thermal degradation of lignin can be explained by the different oxygenated functional groups in their structure, which provides different thermal stabilities^[28]. The thermal degradation of lignin generally occurs in three main steps: 0 to 120 °C, related to the evaporation of absorbed water, 180 to 350 °C, associated with the degradation of carbohydrates, which are converted into volatile gases such as CO, CO₂ and CH₄, and above 350 °C, related to the degradation of lignin-derived products together with the removal of produced gases^[28].

Due to the complexity of lignin's structure, the chemical decomposition of this material involves several competing reactions. Lignin contains several chemical subunits within its macromolecule. During the thermal degradation process, chemical bonds of different bond energies are broken^[23,26,27].

The dehydration of lignin prevails in its thermal degradation pathways. Dehydration of the lignin structure results in pyrolysis products with unsaturated side chains^[28]. Carbon monoxide, carbon dioxide, and methane are also formed during these processes^[29,30]. The decomposition of aromatic rings occurs above 400 °C^[31]. Prolonged heating above 400 °C leads to saturation of aromatic rings, the disruption of C-C bonds, and the release of smaller molecules, such as water, CO₂, and CO, accompanied by the rearrangement and condensation of the aromatic rings within the lignin structural units^[29].

Figure 1a shows a plot of the first derivative of the mass loss versus temperature for the KL and ML samples. One can conclude that the KL sample is thermally more stable than the ML sample due to the highest temperature of maximum weight loss related to the lignin carbohydrate degradation appeared at 320 °C for the ML sample but appeared in the interval between 320 °C to 380 °C for the KL sample.

According to Kindsigo and Kallas^[32], at ambient temperature in the presence of oxygen and water, it is possible to observe the degradation of lignin via wet oxidation, which is increased with elevated temperatures. In the analyzed temperature range of 110-190 °C, the lignin degradation was 20% at 110 °C and 53% at 190 °C; thus, it is expected that at higher temperatures the degradation rate would continue to increase. In this way, the chemical modification

of lignin through carboxylate anion incorporation favors the incorporation of water molecules into its structure due to the higher hydrophilicity of the carboxylated lignin sample (ML sample), making it more unstable and resulting in faster degradation. The total mass losses of the KL and ML samples when heated to 900 °C were 96 wt.% and 88 wt.%, respectively. One can also see from Figure 2a that the lignin continued to decompose at temperatures higher than 900 °C.

Figures 1b and 1c compare the TGA curve of PET_R with those of the PET_R/KL (Figure 1b) and PET_R/ML (Figure 1c) blends. The results of the TGA measurements demonstrate that the admixing of KL and ML into the PET_R to form a blend caused a shift in the onset temperature of thermal degradation (450 °C), whereas the PET_R sample exhibited two mass loss events: the first one in the temperature range of 50 °C to 100 °C (mass loss of 12.5 wt.%) and the second one in the temperature range of 400 °C to 450 °C (mass loss of 75 wt.%). As a consequence, these blends presented a higher residual mass than PET_R (20-25 wt.% versus 12.5 wt.%) at 450 °C.

The increase in the onset temperature of thermal degradation of the PET_R/lignin blends in relation to neat PET_R may be attributed to the chemical compatibility between the PET_R and KL and ML fillers due to the aromatic structure present in both sample types. However, the moisture present in the lignin blends increases the mass loss content in this temperature range, as our results show (see Figure 1a) with degradation temperatures above 450 °C.

3.3 Differential Scanning Calorimetry (DSC)

Figure 2a shows the DSC curves of KL and ML. Typically, the T_g values of unmodified lignins vary from 90 to 180 °C^[33,34]. The significant enthalpy relaxation process that usually occurs in polymers during DSC scanning makes it challenging to determine the T_g value of lignin from the DSC measurements. Complex hydrogen bonding interactions and the highly amorphous structure of kraft lignin favor enthalpy relaxation. This is detected in the interval where a slope change occurs in the heating curve^[35-37]. The T_g values of KL and ML are 100 °C and 127 °C, respectively (Figure 2a). Table 4 summarizes the thermal properties of the studied samples obtained from the DSC measurements, such as the glass transition temperature (T_g), crystallization temperature (T_c), melting

Table 4. DSC results for PET_R and PET/KL and PET/ML blends.

Sample	T _g (°C)*	T _c (°C)*	T _m (°C)*	ΔH _m (J/g)*	X _c (%)*
PET _R	63.30	119.50	253.79	-4.45	3.18%
PET/KF 0.5wt.%	70.29	117.37	257.18	-4.90	3.52%
PET/KF 1.0wt.%	69.70	116.42	256.59	-5.49	3.96%
PET/KF 3.0wt.%	68.34	116.89	256.49	-5.89	4.34%
PET/KF 5.0wt.%	68.80	117.99	253.09	-5.94	4.46%
PET/ML 0.5wt.%	74.96	113.61	255.02	-5.71	4.10%
PET/ML 1.0wt.%	74.76	113.05	258.26	-5.26	3.80%
PET/ML 3.0wt.%	74.77	110.46	258.15	-5.66	4.17%
PET/ML 5.0wt.%	74.98	109.45	256.34	-5.70	4.29%

* T_g, T_c, T_m, ΔH_m and X_c correspond to glass transition temperature, crystallization temperature, melting temperature, melting enthalpy, and degree of crystallinity, respectively.

temperature (T_m), melting enthalpy (ΔH_m), and degree of crystallinity (X_c).

The variation in the values of T_g , T_c , and T_m of the blends in relation to those of PET_R show a clear dependence on both the type and the amount of lignin added. The PET_R sample exhibited T_g , T_c , and T_m values of 63.3, 119.5, and 253.8 °C, respectively, which are typical for this polymer. The DSC curves (Figure 2b, c) for the blends also showed well-defined endothermic peaks of glass transition, exothermic cold crystallization, and endothermic melting peaks, which is characteristic of PET.

In general, PET_R/KL blends exhibited higher T_g and T_m values (approximately 70 °C and 257 °C, respectively) compared with those of PET_R . This shift of the glass and melting transitions to higher temperatures was somewhat larger in the case of PET_R/ML for T_m (approximately 258 °C) and was notably larger for T_g (about 75 °C), except for the PET_R/ML 5.0 wt.% sample. On the whole, the PET_R/ML blends showed more stable melt characteristics (melting temperatures and melting enthalpies) compared to those of the PET_R/KL blends.

The value of T_c presented a maximum decrease in three units (119.5 → 116.4 °C) of temperature for the PET_R/KL 1.0 wt.% blend, while in the PET_R/ML blends, the most significant variation was $T_c = 114 \rightarrow 110$ °C (Table 5). The cold crystallization temperatures of the blends showed an opposite trend from the melting temperatures, where the cold crystallization temperatures of the PET_R/KL and PET_R/ML samples were decreased in comparison to that of PET_R . This temperature reduction was notably larger in the PET_R/ML blends.

The lignin macromolecule contains polar groups capable of producing chemical interactions to become closer to the PET_R chains. These secondary forces may have contributed to the increase of T_g and T_m for the studied blends. The PET_R/ML blends presented higher increases in these two parameters in relation to the PET_R/KL blends, probably due to the incorporation of carboxylate groups in the lignin, favoring its chemical interaction with the PET_R matrix, and consequently, increasing the T_g and T_m values^[38,39].

Miscibility is a crucial parameter to be achieved in polymer blends to improve the properties of homopolymers. In our study, a single T_g was observed in the DSC curves of the blends, which is indicative of miscibility. The polarity of the lignin molecules results in strong interactions between them that hinder their miscibility with other polymers. To maintain miscibility, interaction forces between the polymer matrix (PET in our case) and lignin are required. Generally, PET has the ability to interact with lignin through π electronic interactions favoring the miscibility between them. Hydrogen bonds that eventually form between PET and lignin polar groups also facilitate miscibility. For this reason, lignin surface chemical modification is typically performed to reduce the interaction forces between the lignin molecules, attaching them to hydrophilic polymer matrices, such as PET_R .

The degree of crystallinity is another important property of semi-crystalline thermoplastics that is directly related, among others, to the mechanical properties of plastics. The degree of crystallinity by DSC of the studied blends was assessed using the following Equation 1:

$$X_c = \frac{\Delta H_m - \Delta H_c}{\Delta H_m^0} * 100\% \quad (1)$$

Table 5. Tensile test results for PET_R and PET_R/KL and PET_R/ML blends.

Sample	E (GPa)**	ΔE (GPa)**	σ (Mpa)**	$\Delta\sigma$ (Mpa)**	ϵ_{rup} %**	$\Delta\epsilon_{rup}$ %**
PET_R	1.33	±0.04	57.31	±0.60	NB*	NB*
PET/KF 0.5 wt.%	1.47	±0.06	60.20	±0.85	NB*	NB*
PET/KF 1.0 wt.%	1.55	±0.05	61.62	±0.67	NB*	NB*
PET/KF 3.0 wt.%	1.71	±0.05	39.56	±1.28	2.0	±0.54
PET/KF 5.0 wt.%	1.76	±0.12	37.77	±2.80	2.1	±0.29
PET/ML 0.5 wt.%	1.66	±0.29	20.59	±3.60	0.9	±0.16
PET/ML 1.0 wt.%	1.43	±0.22	20.41	±1.78	1.1	±0.40

*did not break; **E: modulus of elasticity; ΔE : standard deviation of modulus of elasticity; σ : maximum tensile strength; $\Delta\sigma$: standard deviation of maximum tensile strength; ϵ_{rup} : strain at break; $\Delta\epsilon_{rup}$: standard deviation of strain at break.

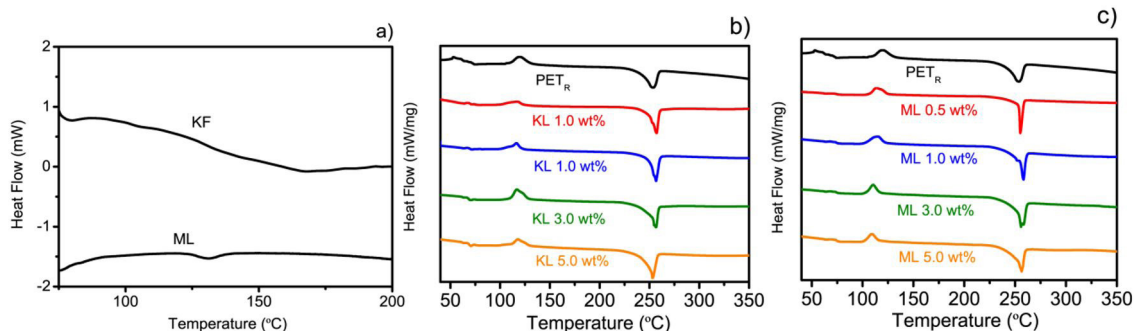


Figure 2. DSC plots for KL and ML (a) lignin; (b-c) PET_R and their respective blends of (b) PET_R/KL and (c) PET_R/ML .

In this equation, the difference between the measured heats of melting, ΔH_m , and the cold crystallization, ΔH_c , define the fusion enthalpy of a sample. The term ΔH_m^0 is a reference value and represents the heat of melting if the polymer were 100% crystalline. The value $\Delta H_m^0 = 140 \text{ J g}^{-1}$ was used^[38].

All samples exhibited low values of X_c (see Table 4). Two different factors could have affected the overall crystallinity of the samples. The first one is related to the production process of the specimens, which was by injection molding. Significant differences between the injection and molding temperatures resulted in a predominantly amorphous sample structure because the polymer chains did not have enough time for periodic ordering. On the other hand, the presence of KL and ML lignin favored the crystallization of PET_R, indicating that lignin acted as a nucleating agent to the PET domains^[39].

3.4 Tensile tests

The results of the mechanical tensile tests, including the modulus of elasticity (E), maximum tensile strength (σ), and strain at break (ϵ_{rup}), are shown in Table 5.

The σ parameter (maximum tensile strength) of a polymer blend indicates the tension transfer capacity from the matrix to the filler, where the higher the interaction between phases, the higher the maximum tensile strength. The chemical modification of lignin did not produce efficient interfacial molecular interactions between the PET and ML components or, consequently, an enhancement in the mechanical properties of the PET_R/ML blends, as is seen from the experimental data (Table 5). Moreover, higher contents of KL in polymer blends (<3.0 wt%) also seemed to be unfavorable for the strength and deformability of the PET_R/KL blends. Formulations containing 3 wt.% and 5 wt.% of ML could not be tested at all, as the mixture of ML with PET_R in these proportions resulted in specimens forming cracks even before the mold was withdrawn.

In contrast, Young's modulus of all PET_R/KL blends followed the fundamental law of mixtures and was nearly the additive function of the composition. On the other hand, lignin, which is more rigid than PET_R, has the capacity to support the applied tension transferred from the polymeric matrix to itself, resulting in a higher Young's module of the respective blends in comparison with PET_R^[40].

Distinct from Young's modulus, the strength, and deformability of blends show more complex behavior. It is generally thought that these characteristics primarily depend on the strength of interfacial adhesion of the components, which is determined, in turn, by the mutual contact surface and the respective strength of interaction^[41]. Water molecules can act as plasticizers to increase the mobility of lignin's polymer chains during its dispersion in the PET_R matrix. There was a much finer dispersion of the KL phase than the ML phase in the respective blends, resulting in a higher contact surface between the KL and PET_R molecules. However, the positive effects of KL on the tensile properties of the PET_R/KL blends seemed to diminish after the content of stiff KL chains exceeded a critical limit. We believe that the analogous critical limit was already attained for the lowest content of ML in the PET_R/ML samples with respect to Young's modulus of the

material. As a result, a decreasing trend in the stiffness of PET_R/ML with the content of ML was observed.

4. Conclusions

In this study, kraft lignin (KL) and chemically modified kraft lignin (ML) were used to produce PET_R/lignin blends. The results of ATR-FTIR, TGA, and DSC analyses verified the presence of chemical modifications in the ML samples. The TGA measurements indicated that KL was thermally more stable than ML, which is intrinsically linked to the ability of ML to absorb water, thus, increasing this material's susceptibility to degradation. Additionally, the water molecule absorption impacts the mechanical properties of the PET_R/lignin blends, making the PET_R/ML blends more fragile than the PET_R/KL blends. The ATR-FTIR spectra of the blends showed no significant differences between them, while the DSC curves exhibited higher glass transition temperatures for the PET_R/lignin blends compared with the PET_R material.

PET_R/KL blends with small amounts of KL (up to approximately 1%) showed improved mechanical properties. Both the modulus of elasticity and the maximum tensile strength of PET_R benefited from the addition of lignin in this situation; this is the expected behavior of compatible polymer blends.

5. Acknowledgements

The authors thank FAPES for a scholarship to Livia Lazzari, Fibria Celulose for supplying the lignin samples, and UFES/LABPETRO for the provision of laboratories and equipment. Leticia Silva and Joyce Araujo thank FAPERJ (grants E-26/201.978/2017 and E-26/202.746/2018) and CNPq (grant 311900/2017-8) for the fellowships.

6. References

- Shah, A. A., Hasan, F., Hameed, A., & Ahmed, S. (2008). Biological degradation of plastics: a comprehensive review. *Biotechnology Advances*, 26(3), 246-265. <http://dx.doi.org/10.1016/j.biotechadv.2007.12.005>. PMID:18337047.
- Vanini, G., Castro, E. V. R., Silva, E. A., Fo., & Romão, W. (2013). Despolimerização química de PET grau garrafa pós-consumo na presença de um catalisador catiônico, o brometo de hexadeciltrimetilamônio (CTAB). *Polímeros: Ciência e Tecnologia*, 23(3), 425-431. <http://dx.doi.org/10.4322/polimeros.2013.084>.
- Abdul Aziz, F. M., Surip, S. N., Bonnia, N. N., & Sekak, K. A. (2018). The effect of pineapple leaf fiber (PALF) incorporation into polyethylene terephthalate (PET) on FTIR, morphology and wetting properties. *IOP Conference Series: Earth and Environmental Science*, 105(1), 012082. <http://dx.doi.org/10.1088/1755-1315/105/1/012082>.
- Gadioli, R., Morais, J. A., Waldman, W. R., & De Paoli, M.-A. (2014). The role of lignin in polypropylene composites with semi-bleached cellulose fibers: mechanical properties and its activity as antioxidant. *Polymer Degradation & Stability*, 108, 23-34. <http://dx.doi.org/10.1016/j.polymdegradstab.2014.06.005>.
- Karmakar, S., De, S. K., & Goswami, A. (2018). A pollution sensitive remanufacturing model with waste items: triangular dense fuzzy lock set approach. *Journal of Cleaner Production*, 187, 789-803. <http://dx.doi.org/10.1016/j.jclepro.2018.03.161>.

6. Karagiannidis, P. G., Stergiou, A. C., & Karayannidis, G. P. (2008). Study of crystallinity and thermomechanical analysis of annealed poly(ethylene terephthalate) films. *European Polymer Journal*, 44(5), 1475-1486. <http://dx.doi.org/10.1016/j.eurpolymj.2008.02.024>.
7. Romão, W., Franco, M. F., Bueno, M. I. M. S., & De Paoli, M.-A. (2010). Distinguishing between virgin and post-consumption bottle-grade poly (ethylene terephthalate) using thermal properties. *Polymer Testing*, 29(7), 879-885. <http://dx.doi.org/10.1016/j.polymtest.2010.05.009>.
8. Romão, W., Franco, M. F., Bueno, M. I. M. S., Eberlin, M. N., & De Paoli, M.-A. (2010). Analysing metals in bottle-grade poly(ethylene terephthalate) by X-ray fluorescence spectrometry. *Journal of Applied Polymer Science*, 117(5), 2993-3000. <http://dx.doi.org/10.1002/app.32232>.
9. Romão, W., Franco, M. F., Corilo, Y. E., Eberlin, M. N., Spinacé, M. A. S., & De Paoli, M.-A. (2009). Poly (ethylene terephthalate) thermo-mechanical and thermo-oxidative degradation mechanisms. *Polymer Degradation & Stability*, 94(10), 1849-1859. <http://dx.doi.org/10.1016/j.polymdegradstab.2009.05.017>.
10. Romão, W., Franco, M. F., Iglesias, A. H., Sanvido, G. B., Mareto, D. A., Gozzo, F. C., Poppi, R. J., Eberlin, M. N., & De Paoli, M.-A. (2010). Fingerprinting of bottle-grade poly(ethylene terephthalate) via matrix-assisted laser desorption/ionization mass spectrometry. *Polymer Degradation & Stability*, 95(4), 666-671. <http://dx.doi.org/10.1016/j.polymdegradstab.2009.11.046>.
11. Abdul Razak, N. C., Inuwa, I. M., Hassan, A., & Samsudin, S. A. (2013). Effects of compatibilizers on mechanical properties of PET/PP blend. *Composite Interfaces*, 20(7), 507-515. <http://dx.doi.org/10.1080/15685543.2013.811176>.
12. Kiziltas, A., Gardner, D. J., Han, Y., & Yang, H.-S. (2011). Thermal properties of microcrystalline cellulose-filled PET-PTT blend polymer composites. *Journal of Thermal Analysis and Calorimetry*, 103(1), 163-170. <http://dx.doi.org/10.1007/s10973-010-0894-6>.
13. Torres-Huerta, A. M., Palma-Ramírez, D., Domínguez-Crespo, M. A., Del Angel-López, D., & de la Fuente, D. (2014). Comparative assessment of miscibility and degradability on PET/PLA and PET/chitosan blends. *European Polymer Journal*, 61, 285-299. <http://dx.doi.org/10.1016/j.eurpolymj.2014.10.016>.
14. Laurichesse, S., & Avérous, L. (2014). Chemical modification of lignins: towards biobased polymers. *Progress in Polymer Science*, 39(7), 1266-1290. <http://dx.doi.org/10.1016/j.progpolymsci.2013.11.004>.
15. Chakar, F. S., & Ragauskas, A. J. (2004). Review of current and future softwood kraft lignin process chemistry. *Industrial Crops and Products*, 20(2), 131-141. <http://dx.doi.org/10.1016/j.indcrop.2004.04.016>.
16. Haddad, M., Bazinet, L., Savadogo, O., & Paris, J. (2017). A feasibility study of a novel electro-membrane based process to acidify Kraft black liquor and extract lignin. *Process Safety and Environmental Protection*, 106, 68-75. <http://dx.doi.org/10.1016/j.psep.2016.10.003>.
17. Luiz, F. S., Scremin, F. R., Werncke, E., Basso, R. L. O., Possan, E., & Bittencourt, P. R. S. (2020). Thermal evaluation by DSC and tensile strength of extruded blends from polyethylene terephthalate and kraft lignin. *Waste and Biomass Valorization*, 11(1), 367-373. <http://dx.doi.org/10.1007/s12649-018-0367-x>.
18. Glasser, W. G., Barnett, C. A., Muller, P. C., & Sarkanen, K. V. (1983). The chemistry of several novel bioconversion lignins. *Journal of Agricultural and Food Chemistry*, 31(5), 921-930. <http://dx.doi.org/10.1021/jf00119a001>.
19. Sahoo, S., Misra, M., & Mohanty, A. K. (2011). Enhanced properties of lignin-based biodegradable polymer composites using injection moulding process. *Composites. Part A, Applied Science and Manufacturing*, 42(11), 1710-1718. <http://dx.doi.org/10.1016/j.compositesa.2011.07.025>.
20. Sameni, J., Krigstin, S., Jaffer, S. A., & Sain, M. (2018). Preparation and characterization of biobased microspheres from lignin sources. *Industrial Crops and Products*, 117, 58-65. <http://dx.doi.org/10.1016/j.indcrop.2018.02.078>.
21. Jeong, H., Park, J., Kim, S., Lee, J., & Cho, J. W. (2012). Use of acetylated softwood kraft lignin as filler in synthetic polymers. *Fibers and Polymers*, 13(10), 1310-1318. <http://dx.doi.org/10.1007/s12221-012-1310-6>.
22. Kadla, J. F., & Kubo, S. (2004). Lignin-based polymer blends: analysis of intermolecular interactions in lignin-synthetic polymer blends. *Composites. Part A, Applied Science and Manufacturing*, 35(3), 395-400. <http://dx.doi.org/10.1016/j.compositesa.2003.09.019>.
23. Silva, L. G., Ruggiero, R., Gontijo, P. M., Pinto, R. B., Royer, B., Lima, E. C., Fernandes, T. H. M., & Calvete, T. (2011). Adsorption of Brilliant Red 2BE dye from water solutions by a chemically modified sugarcane bagasse lignin. *Chemical Engineering Journal*, 168(2), 620-628. <http://dx.doi.org/10.1016/j.cej.2011.01.040>.
24. Edge, M., Wiles, R., Allen, N. S., McDonald, W. A., & Mortlock, S. V. (1996). Characterisation of the species responsible for yellowing in melt degraded aromatic polyesters—I: yellowing of poly(ethylene terephthalate). *Polymer Degradation & Stability*, 53(2), 141-151. [http://dx.doi.org/10.1016/0141-3910\(96\)00081-X](http://dx.doi.org/10.1016/0141-3910(96)00081-X).
25. Silverstein, R. M., Webster, F. X., Kiemle, D. J., & Bryce, D. L. (2014). *Spectrometric identification of organic compounds*. Hoboken: John Wiley & Sons.
26. Grandmaison, J. L., Thibault, J., Kaliaguine, S., & Chantal, P. D. (1987). Fourier-transform infrared spectrometry and thermogravimetry of partially converted lignocellulosic materials. *Analytical Chemistry*, 59(17), 2153-2157. <http://dx.doi.org/10.1021/ac00144a031>.
27. Jakab, E., Faix, O., & Till, F. (1997). Thermal decomposition of milled wood lignins studied by thermogravimetry/mass spectrometry. *Journal of Analytical and Applied Pyrolysis*, 40-41, 171-186. [http://dx.doi.org/10.1016/S0165-2370\(97\)00046-6](http://dx.doi.org/10.1016/S0165-2370(97)00046-6).
28. Brebu, M., & Vasile, C. (2010). Thermal degradation of lignin: a review. *Cellulose Chemistry and Technology*, 44(9), 353-363.
29. Hoareau, W., Trindade, W. G., Siegmund, B., Castellán, A., & Frollini, E. (2004). Sugar cane bagasse and curaua lignins oxidized by chlorine dioxide and reacted with furfuryl alcohol: characterization and stability. *Polymer Degradation & Stability*, 86(3), 567-576. <http://dx.doi.org/10.1016/j.polymdegradstab.2004.07.005>.
30. Meier, D., & Faix, O. (1999). State of the art of applied fast pyrolysis of lignocellulosic materials: a review. *Bioresource Technology*, 68(1), 71-77. [http://dx.doi.org/10.1016/S0960-8524\(98\)00086-8](http://dx.doi.org/10.1016/S0960-8524(98)00086-8).
31. Rohella, R. S., Sahoo, N., Paul, S. C., Choudhury, S., & Chakravorty, V. (1996). Thermal studies on isolated and purified lignin. *Thermochimica Acta*, 287(1), 131-138. [http://dx.doi.org/10.1016/0040-6031\(96\)02983-8](http://dx.doi.org/10.1016/0040-6031(96)02983-8).
32. Kindsigo, M., & Kallas, J. (2006). Degradation of lignins by wet oxidation: model water solutions. *Proceedings of the Estonian Academy of Sciences: Chemistry*, 55(3), 132-144.
33. Irvine, G. M. (1985). The significance of the glass transition of lignin in thermomechanical pulping. *Wood Science and Technology*, 19(2), 139-149. <http://dx.doi.org/10.1007/BF00353074>.
34. Lisperguer, J., Perez, P., & Urizar, S. (2009). Structure and thermal properties of lignins: characterization by infrared spectroscopy and differential scanning calorimetry. *Journal*

- of the Chilean Chemical Society, 54(4), 460-463. <http://dx.doi.org/10.4067/S0717-97072009000400030>.
35. Awal, A., & Sain, M. (2013). Characterization of soda hardwood lignin and the formation of lignin fibers by melt spinning. *Journal of Applied Polymer Science*, 129(5), 2765-2771. <http://dx.doi.org/10.1002/app.38911>.
36. Cachet, N., Camy, S., Benjelloun-Mlayah, B., Condoret, J.-S., & Delmas, M. (2014). Esterification of organosolv lignin under supercritical conditions. *Industrial Crops and Products*, 58, 287-297. <http://dx.doi.org/10.1016/j.indcrop.2014.03.039>.
37. Gordobil, O., Delucis, R., Egüés, I., & Labidi, J. (2015). Kraft lignin as filler in PLA to improve ductility and thermal properties. *Industrial Crops and Products*, 72, 46-53. <http://dx.doi.org/10.1016/j.indcrop.2015.01.055>.
38. Canevarolo, S. V. (2010). *Ciência dos polímeros: um texto básico para tecnólogos e engenheiros*. São Paulo: Artliber
39. Wellen, R. M. R., Canedo, E. L., & Rabello, M. S. (2012). Effect of styrene-co-acrylonitrile on cold crystallization and mechanical properties of poly(ethylene terephthalate). *Journal of Applied Polymer Science*, 125(4), 2701-2710. <http://dx.doi.org/10.1002/app.36585>.
40. Araujo, J. R., Mano, B., Teixeira, G. M., Spinacé, M. A. S., & De Paoli, M.-A. (2010). Biomicrofibrillar composites of high density polyethylene reinforced with curauá fibers: Mechanical, interfacial and morphological properties. *Composites Science and Technology*, 70(11), 1637-1644. <http://dx.doi.org/10.1016/j.compscitech.2010.06.006>.
41. Makkam, S., & Harnnarongchai, W. (2014). Rheological and mechanical properties of recycled PET modified by reactive extrusion. *Energy Procedia*, 56, 547-553. <http://dx.doi.org/10.1016/j.egypro.2014.07.191>.

Received: Dec. 04, 2018

Revised: Aug. 03, 2019

Accepted: Oct. 03, 2019

Supplementary Material

Supplementary material accompanies this paper.

Figure S1. (a) ATR-FTIR spectra of lignin obtained by the kraft process (KL) and chemically modified lignin (ML); (b) PETR/kraft lignin (KL) blends; (c) PETR/modified lignin (ML) blends.

Table S1. Assignments of FTIR bands for PETR and their respective PETR/KL and PETR/ML blends [2-4].

This material is available as part of the online article from <http://www.scielo.br/po>